



Cite this: *Phys. Chem. Chem. Phys.*,
2015, 17, 11198

Energetics of sodium–calcium exchanged zeolite A

H. Sun,^a D. Wu,^b X. Guo,^b B. Shen^a and A. Navrotsky^{*b}

A series of calcium-exchanged zeolite A samples with different degrees of exchange were prepared. They were characterized by powder X-ray diffraction (XRD) and differential scanning calorimetry (DSC). High temperature oxide melt drop solution calorimetry measured the formation enthalpies of hydrated zeolites CaNa-A from constituent oxides. The water content is a linear function of the degree of exchange, ranging from 20.54% for Na-A to 23.77% for 97.9% CaNa-A. The enthalpies of formation (from oxides) at 25 °C are -74.50 ± 1.21 kJ mol⁻¹ TO₂ for hydrated zeolite Na-A and -30.79 ± 1.64 kJ mol⁻¹ TO₂ for hydrated zeolite 97.9% CaNa-A. Dehydration enthalpies obtained from differential scanning calorimetry are 32.0 kJ mol⁻¹ H₂O for hydrated zeolite Na-A and 20.5 kJ mol⁻¹ H₂O for hydrated zeolite 97.9% CaNa-A. Enthalpies of formation of Ca-exchanged zeolites A are less exothermic than for zeolite Na-A. A linear relationship between the formation enthalpy and the extent of calcium substitution was observed. The energetic effect of Ca-exchange on zeolite A is discussed with an emphasis on the complex interactions between the zeolite framework, cations, and water.

Received 24th February 2015,
Accepted 20th March 2015

DOI: 10.1039/c5cp01133g

www.rsc.org/pccp

1. Introduction

Due to their unique compositional and structural diversity, uniform pores with controllable size, and abundant internal area with ordered surfaces and exchangeable mobile cationic zeolites are widely used in industrial and environment processes, including selective adsorption, separation, purification, ion exchange, shape selective catalysis, food production, biochemical engineering and medicine.^{1–4} In almost all application fields, the energetic stability, degree of hydration and interactions related to extra-framework cations are crucial for optimizing the function.

The basic structural unit of zeolite A is a truncated octahedron which is also a sodalite or beta cage.^{5,6} These sodalite units are linked through four-member prisms, forming the unit cell containing 24 tetrahedra (12AlO₄ and 12SiO₄). The central cavity (alpha cage) has a free diameter of 11.4 Å, which can be directly accessed by guests, such as cations and water, through the six 8-member oxygen-ring with an aperture diameter of 4.3 Å.^{7–9}

Owing to the great solubility and availability of sodium salts, direct hydrothermal synthesis of zeolite A usually results in samples in their sodium forms, which can be further modified by replacing the charge-balancing sodium ions by various other cations, including protons. Typically, post-synthesis ion exchange with other alkali and alkaline metal cations may modify the

aperture/pore size of zeolite A, improving its accessibility and catalytic performance in industrial applications. Zeolite K-A has been widely used for dehydration of gases and alcohols.¹⁰ Zeolite Na-A is applied in propylene/propane separation¹¹ and air separation for production of nitrogen.¹² Zeolite Ca-A has shown great performance in selective adsorption separation of normal paraffins from branched chain and cyclic paraffins.¹³ The diffusivities in zeolite molecular sieves can be adjusted by ion exchange to enhance kinetic selective separation.⁸ Transition metal exchanged zeolite A can provide Brønsted sites employed in acid catalysis.¹⁴ In turn, the extra-framework cations also significantly influence the energetics and structural stability of the zeolite frameworks.^{15,16} The cations may also act as precursors to obtain new zeolite frameworks.¹⁷ Therefore, understanding the underlying thermodynamic properties defining the structure, stability, phase evolution and cation–water–framework interactions is fundamentally important for the synthesis and industrial development of zeolites.¹⁸

Enthalpies of formation and transformation are very useful thermochemical parameters describing the energetics of zeolites, which provide insights into structural stability, bonding, and driving force for formation and transition of a given zeolite.¹⁹ High temperature oxide melt drop solution calorimetry can provide accurate thermochemical data for many inorganic materials including nano-phase oxides, nitrides, ceramics, minerals and zeolites.^{19–22} The enthalpies of formation/hydration of various zeolites have already been successfully determined and the energetics of inclusion of cation guests in natural or synthetic zeolite frameworks has been investigated and the relationship between energetics and ionic

^a State Key Laboratory of Chemical Engineering, East China University of Science and Technology, Shanghai 200237, P. R. China

^b Peter A. Rock Thermochemistry Laboratory and NEAT ORU, University of California, Davis, California, 95616, USA. E-mail: anavrotsky@ucdavis.edu

potential has been discussed. However, the energetics of zeolite A with different degrees of calcium exchange is not yet documented.

We employed high temperature oxide melt solution calorimetry to study the energetics of sodium–calcium exchanged zeolites A. Ca-exchanged samples were prepared by ion-exchange of zeolite Na-A in calcium chloride solution of various concentrations (0.05 to 0.25 M). Our objective is to reveal the energetic insights of zeolite A as the composition of extra-framework cation varies, and to understand the interactions between the zeolite A framework, its included cations, and confined water.

2. Experimental methods

2.1. Sample preparation, structural and chemical analyses

The sample preparation procedure, detailed structural and chemical analyses of the same set of hydrated Ca-exchanged zeolite A, including powder X-ray diffraction (XRD), electron microprobe analysis (EMPA) and thermogravimetric analysis (TGA), have been published elsewhere,^{5,6} so we do not repeat them here.

2.2. Differential scanning calorimetry

Differential scanning calorimetry (DSC) was performed on a Netzsch STA 449 system to determine the energetics of dehydration. Pellets weighing about 20 mg were placed in a platinum crucible and heated under an argon flow (40 ml min⁻¹) from 30 to 1200 °C (10 °C min⁻¹). The dehydration enthalpies with respect to liquid water were derived from integration of DSC peaks and correcting for the enthalpy of water vaporization.

2.3. Calorimetry

High temperature oxide melt drop solution calorimetry was performed using a custom-built Calvet twin microcalorimeter. This method has been applied to obtain the energetics of various zeolite frameworks.¹⁹ The methodology has been

described by Navrotsky.^{21,22} Molten lead borate (2PbO·B₂O₃) at 704 °C was used as a solvent. Samples were pressed into pellets (~5 mg) and dropped at room temperature into the molten solvent in the calorimeter under an argon flow (100 ml min⁻¹) to expel any evolved water vapor. This measurement was repeated 6 to 8 times on each sample to ensure reproducibility. The calorimeter was calibrated using the known heat content of corundum pellets. Formation enthalpy is calculated using thermodynamic cycles given in Table 1.

3. Results

3.1. Structure and composition of hydrated zeolites Na-A and CaNa-A

The powder XRD patterns of Ca-exchanged zeolites A are shown in Fig. 1.⁶ All samples are confirmed to be of single phase. Noticeable differences at specific diffraction positions are found as the degree of calcium exchange varies. The present observations correspond well with a previous report,^{2,3} which

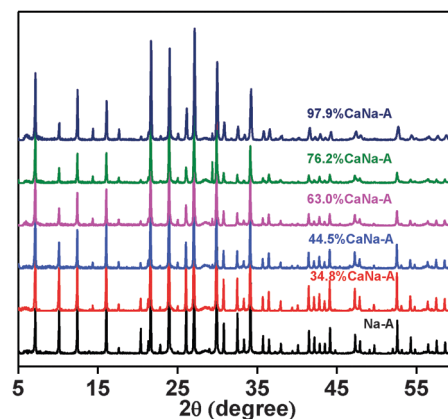


Fig. 1 Powder XRD patterns of zeolites Na-A and CaNa-A. Values in front of CaNa-A denote the degrees of exchange.⁶

Table 1 Thermodynamic cycles for formation enthalpies of zeolites Na-A and CaNa-A from oxides^a

Enthalpy of formation of zeolite Na-A	
$x/2\text{Na}_2\text{O} (\text{soln.}, 704\text{ °C}) + y/2\text{Al}_2\text{O}_3 (\text{soln.}, 704\text{ °C}) + z\text{SiO}_2 (\text{soln.}, 704\text{ °C}) + m\text{H}_2\text{O} (\text{soln.}, 704\text{ °C}) \rightarrow \text{Na}_x\text{Al}_y\text{Si}_z\text{O}_2 \cdot m\text{H}_2\text{O} (\text{s}, 25\text{ °C})$	$\Delta H_1 = \Delta H_{\text{ds-hyd}}$
$\text{Na}_2\text{O} (\text{s}, 25\text{ °C}) \rightarrow \text{Na}_2\text{O} (\text{soln.}, 704\text{ °C})$	ΔH_2
$\text{Al}_2\text{O}_3 (\text{s}, 25\text{ °C}) \rightarrow \text{Al}_2\text{O}_3 (\text{soln.}, 704\text{ °C})$	ΔH_3
$\text{SiO}_2 (\text{s}, 25\text{ °C}) \rightarrow \text{SiO}_2 (\text{soln.}, 704\text{ °C})$	ΔH_4
$\text{H}_2\text{O} (\text{l}, 25\text{ °C}) \rightarrow \text{H}_2\text{O} (\text{soln.}, 704\text{ °C})$	ΔH_5
$x/2\text{Na}_2\text{O} (\text{s}, 25\text{ °C}) + y/2\text{Al}_2\text{O}_3 (\text{s}, 25\text{ °C}) + z\text{SiO}_2 (\text{s}, 25\text{ °C}) + m\text{H}_2\text{O} (\text{l}, 25\text{ °C}) \rightarrow \text{Na}_x\text{Al}_y\text{Si}_z\text{O}_2 \cdot m\text{H}_2\text{O} (\text{s}, 25\text{ °C})$	$\Delta H_6 = \Delta H_{\text{f-hyd,ox}}$
$\Delta H_6 = \Delta H_1 + x/2\Delta H_2 + y/2\Delta H_3 + z\Delta H_4 + m\Delta H_5$	

Enthalpy of formation of zeolite CaNa-A	
$a/2\text{Na}_2\text{O} (\text{soln.}, 704\text{ °C}) + b\text{CaO} (\text{soln.}, 704\text{ °C}) + c/2\text{Al}_2\text{O}_3 (\text{soln.}, 704\text{ °C}) + d\text{SiO}_2 (\text{soln.}, 704\text{ °C}) + n\text{H}_2\text{O} (\text{g}, 704\text{ °C}) \rightarrow$	$\Delta H_7 = \Delta H_{\text{ds-hyd}}$
$\text{Na}_a\text{Ca}_b\text{Al}_c\text{Si}_d\text{O}_2 \cdot n\text{H}_2\text{O} (\text{s}, 25\text{ °C})$	
$\text{Na}_2\text{O} (\text{s}, 25\text{ °C}) \rightarrow \text{Na}_2\text{O} (\text{soln.}, 704\text{ °C})$	ΔH_2
$\text{Al}_2\text{O}_3 (\text{s}, 25\text{ °C}) \rightarrow \text{Al}_2\text{O}_3 (\text{soln.}, 704\text{ °C})$	ΔH_3
$\text{SiO}_2 (\text{s}, 25\text{ °C}) \rightarrow \text{SiO}_2 (\text{soln.}, 704\text{ °C})$	ΔH_4
$\text{H}_2\text{O} (\text{l}, 25\text{ °C}) \rightarrow \text{H}_2\text{O} (\text{soln.}, 704\text{ °C})$	ΔH_5
$\text{CaO} (\text{s}, 25\text{ °C}) \rightarrow \text{CaO} (\text{soln.}, 704\text{ °C})$	ΔH_8
$a/2\text{Na}_2\text{O} (\text{s}, 25\text{ °C}) + b\text{CaO} (\text{s}, 25\text{ °C}) + c/2\text{Al}_2\text{O}_3 (\text{s}, 25\text{ °C}) + d\text{SiO}_2 (\text{s}, 25\text{ °C}) + n\text{H}_2\text{O} (\text{l}, 25\text{ °C}) \rightarrow \text{Na}_a\text{Ca}_b\text{Al}_c\text{Si}_d\text{O}_2 \cdot n\text{H}_2\text{O} (\text{s}, 25\text{ °C})$	$\Delta H_9 = \Delta H_{\text{f-hyd,ox}}$
$\Delta H_9 = \Delta H_7 + a/2\Delta H_2 + b\Delta H_8 + c/2\Delta H_3 + d\Delta H_4 + n\Delta H_5$	

^a ΔH_1 and ΔH_7 are the drop solution enthalpies of zeolites; ΔH_2 , ΔH_3 , ΔH_4 , ΔH_5 , and ΔH_8 are the drop solution enthalpies of oxides and liquid water; ΔH_6 and ΔH_9 are the formation enthalpies of zeolites from oxides.

shows that the lattice parameter a is closely related to the calcium content in Ca-exchanged zeolites A. The chemical compositions and the calculated molar mass (per mole TO_2) of Ca-exchanged zeolites A were detailed in our previous work.^{5,6} The Si/Al ratio of all samples is identical (1.03 ± 0.01), which is very close to that of the ideal zeolite A. This is a strong indication of consistent high framework quality after ion-exchange. The degree of Ca-exchange ranges from 34.8 to 97.9%. TGA data for all samples show a similar weight loss behavior corresponding to framework dehydration. The hydration level increases as the degree of Ca-exchange increases. Similar trends were also observed for other Ca-exchanged zeolites.²³

3.2. Differential scanning calorimetry (DSC)

The DSC traces of Ca-exchanged zeolites A are presented in Fig. 2. Considering the structural collapse of zeolite A at temperatures higher than 800 °C, here we mainly focused on events below 800 °C. The major broad endothermic peaks below 800 °C correspond to framework dehydration. These peaks tend to shift to a higher temperature with increasing Ca content. We estimated the dehydration enthalpy of zeolite A to form liquid water ($\Delta H_{\text{deh,l}}$) by integration of the broad DSC peaks ($\Delta H_{\text{integral}}$ from 30 to approximately 250 °C) and subtracting the heat of vaporization of water ($\Delta H_{\text{vap-water}}$; see Fig. 3). The calculation can be expressed as $\Delta H_{\text{deh,l}} = \Delta H_{\text{integral}} - \Delta H_{\text{vap-water}}$. Zeolite Na-A presents the most endothermic dehydration enthalpy ($32.0 \text{ kJ mol}^{-1} \text{ H}_2\text{O}$), which is supported by the results of reaction calorimetry ($29.0 \text{ kJ mol}^{-1} \text{ H}_2\text{O}$),²⁴ while the sample 97.9% CaNa-A is least endothermic ($20.5 \text{ kJ mol}^{-1} \text{ H}_2\text{O}$).

3.3. Calorimetry

The enthalpies of formation of Ca-exchanged zeolites A at 25 °C from constituent oxides ($\Delta H_{\text{f-hyd,ox}}$) and elements ($\Delta H_{\text{f-hyd,el}}$) were calculated from drop solution enthalpies ($\Delta H_{\text{ds-hyd}}$) of hydrated zeolite samples using the thermodynamic cycles in Table 1. ΔH_{ds} values of constituent oxides used in the thermodynamic cycle are summarized in Table 2. Table 3 lists the calculated enthalpies of formation. The enthalpy of formation from oxides increases (becomes less exothermic) as the degree of Ca-exchange increases.

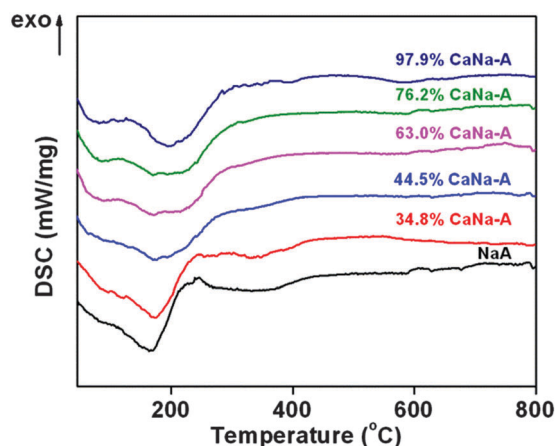


Fig. 2 DSC curves of zeolites Na-A and CaNa-A.

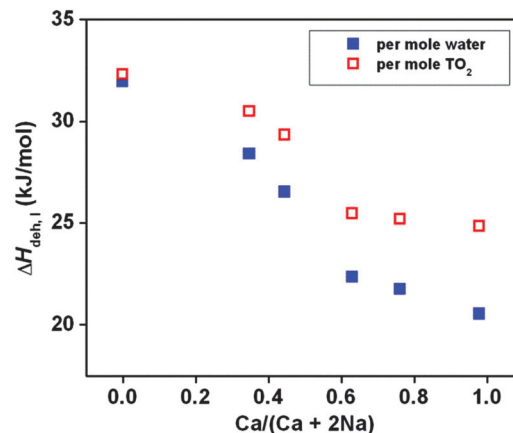


Fig. 3 Dehydration enthalpy of zeolites Na-A and CaNa-A vs. mole fraction of calcium.

Table 2 Drop solution enthalpies for constituent oxides and water in molten lead borate at 704 °C and formation enthalpies from elements at 25 °C^a

Zeolite	ΔH_{ds} (kJ mol^{-1})	$\Delta H_{\text{f,el}}$ (kJ mol^{-1})
Sodium oxide (Na_2O)	-113.10 ± 0.83^{26}	-414.84 ± 0.25^{27}
Calcium oxide (CaO)	-17.49 ± 1.21^{28}	-635.09 ± 0.96^{27}
Corundum (Al_2O_3)	107.93 ± 0.98^{28}	-1675.69 ± 1.20^{27}
Quartz (SiO_2)	39.13 ± 0.32^{28}	-910.85 ± 1.70^{27}
Water (H_2O)	68.98 ± 0.10^{27}	-285.08 ± 0.10^{27}

^a Ref. 26–28.

Table 3 Enthalpies of drop solution and formation (25 °C) of hydrated zeolites Na-A and CaNa-A (on mole TO_2 basis)

Zeolite	$\Delta H_{\text{ds-hyd}}^a$ (kJ mol^{-1})	$\Delta H_{\text{f-hyd,ox}}^b$ (kJ mol^{-1})	$\Delta H_{\text{f-hyd,el}}^c$ (kJ mol^{-1})
Na-A	$163.54 \pm 1.15(6)^d$	-74.50 ± 1.21	-1426.37 ± 1.48
34.8% CaNa-A	$162.32 \pm 1.24(6)^d$	-60.03 ± 1.28	-1455.21 ± 1.55
44.5% CaNa-A	$159.43 \pm 1.49(6)^d$	-54.94 ± 1.54	-1481.90 ± 1.76
63.0% CaNa-A	$155.03 \pm 1.16(6)^d$	-42.97 ± 1.22	-1489.99 ± 1.48
76.2% CaNa-A	$158.90 \pm 1.72(8)^d$	-42.91 ± 1.76	-1512.58 ± 1.96
97.9% CaNa-A	$155.70 \pm 1.58(6)^d$	-30.79 ± 1.64	-1536.47 ± 1.84

^a Drop solution enthalpy of hydrated zeolites. ^b Formation enthalpy of hydrated zeolites from oxides. ^c Formation enthalpy of hydrated zeolites from elements. ^d The values in parentheses denote the number of measurements.

Zeolite Na-A has the most exothermic formation enthalpy of $-74.50 \pm 1.21 \text{ kJ mol}^{-1} \text{ TO}_2$, which is in good agreement with the previously measured value ($-74.24 \pm 0.65 \text{ kJ mol}^{-1} \text{ TO}_2^{25}$), while zeolite 97.9% CaNa-A possesses the least exothermic formation enthalpy of $-30.79 \pm 1.64 \text{ kJ mol}^{-1} \text{ TO}_2$.

4. Discussion

Since all the samples were equilibrated under the same conditions, the degree of hydration reflects the nature of zeolite A and indicates the interactions of water molecules with the frameworks. The framework features two types of interconnected channels, the sodalite cages have a window diameter of 2.8 Å,

comparable to that of water; and the central cavities are both larger and water accessible. The confined water can be removed, by heating and/or evacuation, without affecting the framework structure. The weight loss observed in TG curves includes two forms of water: molecular water in the void space and more tightly bound water, likely hydroxyl on the surface. Most of the molecular water is liberated below 450 °C, whereas the hydroxyl water can only be extracted above 450 °C.²⁹ The weight loss in this region (> 450 °C) for all samples ranges from 0.3 to 2.0%, indicating that zeolites A have low surface hydroxyl concentrations. In each zeolite A unit cell, there are twelve net negative charges, which have to be balanced by the positive guest ions.³⁰ These high energy sites have their distinct crystallographic positions and are classified into three categories: site I, centered in the six-member rings and displaced into the alpha cavity; site II, located near the center of the eight-member rings and being close to its planes, and site III, centered in the four-member rings and displaced into the alpha cavity. Accordingly, the charge-balancing sodium cations in zeolite Na-A are not randomly dispersed, but rather sit on the twelve well-arranged "chairs", which can be occupied by other cationic guests such as the calcium ions as well. Specifically, eight of them prefer site I, the other three are located on site II, and the remaining one is bonded on site III. The site selectivity for sodium cations ranks in the order of I > II > III.³¹ When a water molecule enters the void space of zeolite A, it may interact with the extra, charge-balancing cations, compete with the pre-adsorbed water molecules, and bind to the oxygen atoms embedded in the structure. Despite, or perhaps because of, these multiple possible mechanisms, the extra-framework cation-water interactions present the dominant energetic effect on the hydration of zeolite A.³²

The interaction of water with ion-exchanged zeolites is a complex event involving multiple parameters. The results of our current work highlight the cation effect. A theoretical study on water adsorption in zeolite Na-A suggests that there are 28 water molecules confined/adsorbed in an ideal unit cell when it is fully hydrated.³² Our work supports this conclusion by providing directly measured values ranging from 24.3 to 29.0 molecules per unit cell. Specifically, structural studies³² show that twenty water molecules construct a distorted dodecahedron in the central cavity (α -cage), four self-assemble into a distorted tetrahedron in the sodalite cage, three are bound to sodium ions at sites II, and the remaining one interacts with sodium ions at site III. In addition, the binding energies of various positions with water are calculated to be less strong in the following order, Na⁺ (III) > Na⁺ (II) > α -cage > β -cage, 78.40 kJ mol⁻¹ H₂O for Na⁺ (III) and 20.22 kJ mol⁻¹ H₂O for β -cage.³² In other words, the sodium cations at site III show the strongest interaction with water, while the β -cage has the weakest. However, once two monovalent sodium cations are replaced by one divalent calcium cation, the positions of cations are structurally and thermodynamically adjusted. An extreme condition is that when sodium is fully exchanged with calcium, three out of eight sites I, two out of three sites II, and site III are cation-vacant.³³ As a result, only a minority of the water

molecules are able to directly interact with the cation sites. Hence, the overall enthalpies of dehydration are less endothermic (see Fig. 3) as the Ca content increases. Previous work on ion-exchanged chabazite³⁴ points out that water-zeolite interactions tend to decrease upon increasing hydration, which means the enthalpy of hydration is most exothermic for very low water loading and it becomes less exothermic as the hydration level increases. The present study on ion exchanged zeolite A further confirms and supports this conclusion.

The formation enthalpy, $\Delta H_{f,\text{hyd,ox}}$, of hydrated zeolites A at 25 °C from constituent oxides can be divided into two parts: $\Delta H_{f,\text{deh,ox}}$ and $\Delta H_{\text{hyd,l}}$ ($-\Delta H_{\text{deh,l}}$). $\Delta H_{f,\text{deh,ox}}$ refers to the formation enthalpy of the corresponding dehydrated zeolites A at 25 °C from constituent oxides, while $\Delta H_{\text{hyd,l}}$ is the hydration enthalpy of the same dehydrated zeolites A at 25 °C relative to liquid water. $\Delta H_{f,\text{deh,ox}}$ of zeolites is closely linked to the energetics of their framework structures. Formation enthalpies of dehydrated zeolites A are derived from the measured formation enthalpies of hydrated zeolites A and the estimated hydration enthalpies from DSC analysis.

Formation enthalpies of hydrated zeolites A are plotted against the mole fraction of calcium and the average ionic potential, Z/r , the ratio of average charge to the mean radius of a mixture of ions of each sample (see Fig. 4). In addition, the

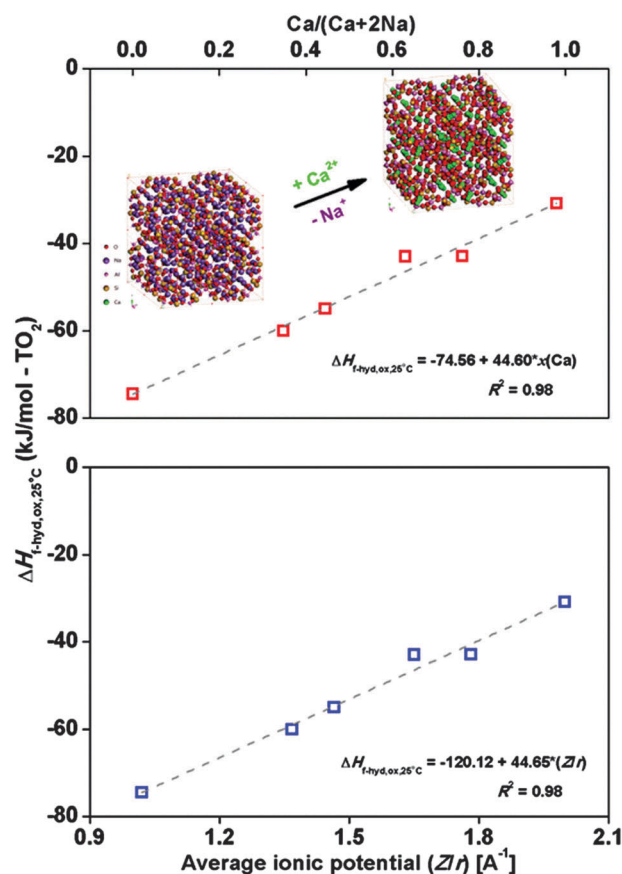


Fig. 4 Formation enthalpy of hydrated zeolites Na-A and CaNa-A from oxides vs. mole fraction of calcium and average ionic potential. Points denote the measured results and dashed lines show the fitted linear trends.

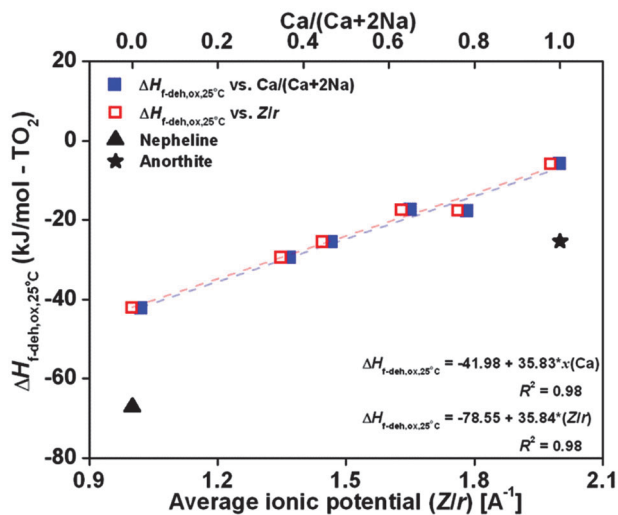


Fig. 5 Formation enthalpy of dehydrated zeolites Na-A and CaNa-A from oxides vs. mole fraction of calcium and average ionic potential. Points denote the measured results and dashed lines show the fitted linear trends.

obtained enthalpies of formation of dehydrated zeolites A are plotted in Fig. 5. As the average ionic potential increases, the formation enthalpies become less exothermic linearly. This positive linear trend is consistent with previous studies on zeolites Y, beta, and natrolite, all of which show less exothermic formation enthalpies from oxides for both hydrated and dehydrated zeolites as the average ionic potential increases.^{35–38} This reflects the fundamental acid–base chemistry of ternary oxide formation, with alkali ternary oxide compounds showing more exothermic enthalpies of formation than alkaline earth compounds.

Zeolite A is metastable with respect to its dense phase (Na-A to nepheline³⁹ and Ca-A to anorthite⁴⁰). The formation enthalpies of these dense phases were determined to be $-67.20 \pm 2.04 \text{ kJ mol}^{-1} \text{ TO}_2$ for nepheline and $-25.45 \pm 0.79 \text{ kJ mol}^{-1} \text{ TO}_2$ for anorthite,⁴¹ which are more exothermic than that of the zeolites A obtained in this work (Fig. 5). This difference in formation energy represents the instability of synthetic zeolites relative to their corresponding dense phase natural minerals, which can be relaxed through spontaneous amorphization,³⁹ recrystallization⁴² and/or other types of phase transformation under alkaline hydrothermal conditions.⁴³

5. Conclusions

Zeolites CaNa-A with calcium contents ranging from 0 to 97.9% were prepared and characterized. Energetics of Ca-exchanged zeolites A was studied using high temperature oxide melt drop solution calorimetry. Crystallographic analysis (XRD) suggests structural evolution as a function of Ca-exchange. The water content of zeolites CaNa-A exhibits a positive linear trend as the degree of Ca-exchange increases. The dehydration enthalpies monotonically decline with increasing calcium content. Substitution of sodium by calcium leads to less exothermic enthalpies of formation, which are a linear function of mole fraction of calcium and average ionic potential.

Author contribution

H.S., D.W. and A.N. designed the research. H.S., D.W. and X.G. performed the experiments. H.S., D.W., X.G., B.S. and A.N. analyzed the data. H.S., D.W. and A.N. wrote the paper jointly, and take full responsibility for the content of the paper.

Acknowledgements

H.S. is grateful to the National Natural Science Foundation of China for the financial support under the National Natural Science Fund for Young Scholar (No. 21201063), the Ministry of Education of Republic of China for the financial support under the Research Fund for the Doctoral Program of Higher Education of China (RFDP) (No. 20110074120020) and the Fundamental Research Funds for the Central Universities, and the China Scholarship Council for the State Scholarship Fund (No. 201308310077). The calorimetric work was supported by the U.S. Department of Energy, Office of Basic Energy Sciences, grant DEFG02-97ER14749.

References

- 1 J. Weitkamp and L. Puppe, *Catalysis and zeolites: fundamentals and applications*, Springer, Heidelberg, 1999.
- 2 S. M. Auerbach, K. A. Carrado and P. K. Dutta, *Handbook of Zeolite Science and Technology*, Taylor & Francis, London, 2003.
- 3 A. Corma, *Chem. Rev.*, 1995, **95**, 559–614.
- 4 N. Y. Chen, W. E. Gorwood and F. G. Dwyer, *Shape selective catalysis in industrial applications*, Macel Dekker, Inc., New York, 1996.
- 5 H. Sun, D. Wu, X. Guo and A. Navrotsky, *Phys. Chem. Chem. Phys.*, 2015, **17**, 9241–9247.
- 6 H. Sun, D. Wu, X. F. Guo, B. X. Shen, J. C. Liu and A. Navrotsky, *J. Phys. Chem. C*, 2014, **118**, 25590–25596.
- 7 T. B. Reed and D. W. Breck, *J. Am. Chem. Soc.*, 1956, **78**, 5972–5977.
- 8 D. W. Breck, *Zeolite Molecular Sieves*, Wiley, New York, 1974.
- 9 R. L. Firor and K. Seff, *J. Am. Chem. Soc.*, 1978, **100**, 3091–3096.
- 10 B. Sarkar, K. Sunitha, S. Sridhar and V. Kale, *J. Polym. Mater.*, 2013, **30**, 131–143.
- 11 C. A. Grande and A. E. Rodrigues, *Ind. Eng. Chem. Res.*, 2005, **44**, 8815–8829.
- 12 X. J. Yin, G. S. Zhu, W. S. Yang, Y. S. Li, G. Q. Zhu, R. Xu, J. Y. Sun, S. L. Qiu and R. R. Xu, *Adv. Mater.*, 2005, **17**, 2006–2010.
- 13 J. A. C. Silva and A. E. Rodrigues, *Ind. Eng. Chem. Res.*, 1997, **36**, 3769–3777.
- 14 P. E. Riley and K. Seff, *J. Phys. Chem.*, 1975, **79**, 1594–1601.
- 15 L. Campana, A. Selloni, J. Weber and A. Goursot, *J. Phys. Chem.*, 1995, **99**, 16351–16356.
- 16 J. G. Nery, Y. P. Mascarenhas and A. K. Cheetham, *Microporous Mesoporous Mater.*, 2003, **57**, 229–248.
- 17 M. Yoshikawa, S. I. Zones and M. E. Davis, *Microporous Mater.*, 1997, **11**, 127–136.
- 18 M. E. Davis and R. F. Lobo, *Chem. Mater.*, 1992, **4**, 756–768.

- 19 A. Navrotsky, O. Trofymlyuk and A. A. Levchenko, *Chem. Rev.*, 2009, **109**, 3885–3902.
- 20 A. Navrotsky, *J. Am. Ceram. Soc.*, 2014, **97**, 3349–3359.
- 21 A. Navrotsky, *Phys. Chem. Miner.*, 1997, **24**, 222–241.
- 22 A. Navrotsky, *Phys. Chem. Miner.*, 1977, **2**, 89–104.
- 23 H. Luhrs, J. Derr and R. X. Fischer, *Microporous Mesoporous Mater.*, 2012, **151**, 457–465.
- 24 J. W. Carey and A. Navrotsky, *Am. Mineral.*, 1992, **77**, 930–936.
- 25 S. Turner, J. R. Sieber, T. W. Vetter, R. Zeisler, A. F. Marlow, M. G. Moreno-Ramirez, M. E. Davis, G. J. Kennedy, W. G. Borghard, S. Yang, A. Navrotsky, B. H. Toby, J. F. Kelly, R. A. Fletcher, E. S. Windsor, J. R. Verkouteren and S. D. Leigh, *Microporous Mesoporous Mater.*, 2008, **107**, 252–267.
- 26 I. Kiseleva, A. Navrotsky, I. A. Belitsky and B. A. Fursenko, *Am. Mineral.*, 1996, **81**, 668–675.
- 27 B. S. Hemingway and R. A. Robie, *U.S. Geol. Survey Bull.*, 1995, 2131.
- 28 I. Kiseleva, A. Navrotsky, I. A. Belitsky and B. A. Fursenko, *Am. Mineral.*, 1996, **81**, 658–667.
- 29 I. A. Beta, B. Hunger, W. Bohlmann and H. Jobic, *Microporous Mesoporous Mater.*, 2005, **79**, 69–78.
- 30 D. W. Breck, W. G. Eversole, R. M. Milton, T. B. Reed and T. L. Thomas, *J. Am. Chem. Soc.*, 1956, **78**, 5963–5971.
- 31 K. Ogawa, M. Nitta and K. Aomura, *J. Phys. Chem.*, 1978, **82**, 1655–1660.
- 32 K. O. Koh and M. S. Jhon, *Zeolites*, 1985, **5**, 313–316.
- 33 K. Ogawa, M. Nitta and K. Aomura, *J. Phys. Chem.*, 1979, **83**, 1235–1236.
- 34 S. H. Shim, A. Navrotsky, T. R. Gaffney and J. E. MacDougall, *Am. Mineral.*, 1999, **84**, 1870–1882.
- 35 S. Y. Yang and A. Navrotsky, *Microporous Mesoporous Mater.*, 2000, **37**, 175–186.
- 36 P. P. Sun, S. Deore and A. Navrotsky, *Microporous Mesoporous Mater.*, 2006, **91**, 15–22.
- 37 P. P. Sun and A. Navrotsky, *Microporous Mesoporous Mater.*, 2008, **109**, 147–155.
- 38 L. L. Wu, A. Navrotsky, Y. Lee and Y. Lee, *Microporous Mesoporous Mater.*, 2013, **167**, 221–227.
- 39 C. Kosanovic, B. Subotic and I. Smit, *Thermochim. Acta*, 1998, **317**, 25–37.
- 40 R. Dimitrijevic, V. Dondur and A. Kremenovic, *Zeolites*, 1996, **16**, 294–300.
- 41 A. Navrotsky and Z. R. Tian, *Chem. – Eur. J.*, 2001, **7**, 769–774.
- 42 V. Dondur, N. Petranovic and R. Dimitrijevic, *Mater. Sci. Forum*, 1996, **214**, 91–98.
- 43 B. Subotic and L. Sekovanic, *J. Cryst. Growth*, 1986, **75**, 561–572.